SOCIETY OF PETROLEUM ENGINEERS OF AIME
6200 North Central Expressway
Dallas, Texas 75206

PAPER NUMBER SPE 4257

The Influence of Gas Saturation on Waterflood Performance - Variations Caused by Changes in Flooding Rate

By

Anil K. Dandona and R. A. Morse, Members AIME, Texas A&M U.

ABSTRACT

It has been recognized that the presence of a gas saturation prior to waterflooding can have an important influence on oil recovery. The published results on the subject are derived from laboratory experiments on essentially one-dimensional horizontal systems flooded with low pressure differentials. In field applications, high pressure gradients could cause important effects not noted in the laboratory studies such as the disappearance of part or all of the gas by solution in the oil bank. Also, it has been realized that gravity forces make it impossible to initiate and maintain a uniform gas saturation from top to bottom of the production section.

By the use of numerical models a study has been made of the effects of flooding rate on performance of waterfloods in reservoirs having gas saturation. Flooding rates over a very wide range have been simulated. At very high rates the gas is put into solution in the oil bank ahead of the water so no gas saturation effect is noted. The simulated performance at very low rates in the absence of gravity check very well with the published laboratory data. Introduction of gravity causes markedly different performance from that of the one-dimensional horizontal systems because of the nonuniform vertical distribution of initial gas saturation and gravity effects on the injected water distribution.

References and illustrations at end of paper.

INTRODUCTION

At the present time, a large fraction of the oil originally in place is left unrecovered in oil reservoirs after depletion by the best methods available. The need for added recovery is of equal importance with the search for new oil-producing structures. Waterflooding is, and has been in the past, the most universally used method for increasing oil recovery beyond the levels provided by natural depletion. Improvements of waterflooding should lead to economic recovery of additional oil in substantial quantities. One of the methods that has been proposed for increasing recovery of oil by water displacement involves creating a gas phase ahead of the waterflood front.

As early as 1922, Russell[1] found experimentally that flooding of oil reservoirs by a mixture of water and gas yielded considerably more oil than water or gas drive alone. In the year 1932, producers in the Bradford field injected their surplus produced gas into oil reservoirs to conserve gas. The operators noted that the injection of gas prior to waterflooding resulted in improved oil recoveries. Breston[2] made a survey of various operators in the Bradford and Allegany oil fields and found almost all operators who had injected gas prior to waterflooding thought they had experienced additional oil recoveries beyond those attainable by waterflood alone. However, the exact mechanism by which additional displacement of oil from reservoirs had occurred was not clearly understood.

In the late 40's extensive laboratory work was conducted to study how the presence of a gas saturation caused improved oil recovery by waterflooding. The various factors that were considered responsible for reducing oil saturation or increasing oil recoveries were (1) changes in physical characteristics of oil, (2) Jamin action of gas and (3) additional driving action of gas. Holmgren and Morse[3] showed that the presence of gas saturation caused the oil saturation following water drive to be reduced by as much as 15 percent of pore space below the levels obtained with no gas saturation present. It appeared that, over a range of conditions, gas saturation could be substituted directly for residual oil. Kyte et al.[4] made further investigations into the mechanism of waterflooding in the presence of gas saturation. Kyte noted that, at the beginning of a flood, only gas was produced. Subsequently, gas production ceased and only oil was produced. After water breakthrough, oil and increasing amounts of water were produced simultaneously. He found definite relationships between (1) mobile and trapped gas saturation and (2) residual oil and initial mobil gas saturation.

The effect of the presence of gas on the relative permeabilities during waterflood was investigated by Holmgren and Morse.[3] They found that the presence of gas saturation did not affect the water relative permeability at a given water saturation, but lowered the relative permeability to oil at a given oil saturation.

Today it is an established fact that the presence of a free gas saturation prior to waterflooding can have an important influence on oil recovery.[1-14] Much of the published information on this subject was obtained under conditions that were either not clearly representative of those existing in a reservoir or were not sufficiently controlled to permit evaluation of the effects specifically caused by the presence of gas saturation. The results were derived from laboratory experiments on essentially one-dimensional horizontal systems flooded with low pressure differentials. None of the published results of the research include the effects of gravity while waterflooding in the presence of gas saturation.

Using a numerical model, this paper reports the results of an investigation of the displacement by waterflooding of oil from reservoir rock in the presence of gas saturation. The effects of water injection rates on the performance of waterfloods have been studied in detail. Also included in the study is the effect of gravitational forces on the performance of the process.

PROCEDURE

It has been pointed out by Morse and Whiting[15] that, except for local effects around the producing wells, flow in an oil reservoir can be simulated by a linear system.

For this study a three-fluid phase, two-dimensional numerical model was developed. The model includes the effects of gravity and can be operated as a one- or two-dimensional model.

Following are the equations describing the flow of fluids in a two-dimensional system flowing gas, oil and water.

Gas Equations

$$u_{gx} = - k_x \frac{k_{rgx}}{\mu_g} \left(\frac{\partial p_g}{\partial x}\right) - k_x \frac{k_{rox}}{\mu_o} \left(\frac{\partial p_o}{\partial x}\right) R_s \quad \ldots\ldots (1)$$

$$u_{gz} = -k_z \frac{k_{rgz}}{\mu_g} \left(\frac{\partial p_g}{\partial z} - \rho_g\right) - k_z \frac{k_{roz}}{\mu_o} \left(\frac{\partial p_o}{\partial z} - \rho_o\right) R_s \quad (2)$$

Oil Equations

$$u_{ox} = -k_x \frac{k_{rox}}{\mu_o} \left(\frac{\partial p_o}{\partial x}\right) \ldots\ldots (3)$$

$$u_{oz} = -k_z \frac{k_{roz}}{\mu_o} \left(\frac{\partial p_o}{\partial z} - \rho_o\right) \ldots (4)$$

Water Equations

$$u_{wx} = -k_x \frac{k_{rwx}}{\mu_w} \left(\frac{\partial p_w}{\partial x}\right) \ldots\ldots (5)$$

$$u_{wz} = -k_z \frac{k_{rwz}}{\mu_w} \left(\frac{\partial p_w}{\partial z} - \rho_w\right) \ldots (6)$$

The continuity equations for each of the three phases are as follows.

Gas

$$\frac{\partial}{\partial x}(u_{gx}) + \frac{\partial}{\partial z}(u_{gz}) - q_g = \frac{\partial S_g}{\partial t} \quad \ldots\ldots (7)$$

Oil

$$\frac{\partial}{\partial x}(u_{ox}) + \frac{\partial}{\partial z}(u_{oz}) - q_o = \frac{\partial S_o}{\partial t} \quad (8)$$

Water

$$\frac{\partial}{\partial x}(u_{wx}) + \frac{\partial}{\partial z}(u_{wz}) - q_w = \frac{\partial S_w}{\partial t} \quad (9)$$

Saturation Equation

$$S_o + S_w + S_g = 1.0 \quad \ldots\ldots (10)$$

Capillary Pressure Equations

$$p_g = p_o + p_{c_{g-o}} \quad \ldots\ldots (11)$$

$$p_w = p_o - p_{c_{w-o}} \quad \ldots\ldots (12)$$

All of these equations can be combined to form an expression in terms of oil pressure only. The procedure has been described by Breitenbach *et al.*[16,17] Using the nomenclature of Breitenbach, the final simulation equation is of the following form.

$$O_x^+ \Delta p_x^+ + O_z^+ \Delta p_z^+ + O_x^- \Delta p_x^- + O_z \Delta p_z^- + A9$$
$$= A8\left(\frac{p_{t_1} - p_{t_o}}{t_1 - t_o}\right). \quad \ldots\ldots (13)$$

The pressures were determined at the end of each time step by an implicit solution of Eq. 13. A banded matrix inversion solution technique was used for calculating pressures. After the pressures were known, saturations were calculated explicitly by Eqs. 8 through 10.

Basic capillary pressure and relative permeability characteristics of the reservoir rock for all runs are shown in Figs. 1 through 4. The formula used for calculating capillary pressure between gas and oil is shown in Eq. 14 and that for water and oil by Eq. 15. The water-oil capillary pressure curve is shown in Fig. 1. Gas-oil capillary pressure related to total liquid saturation (oil + water) is identical to oil-water capillary pressure related to water saturation for this study. Relative permeabilities were represented by Formulae 16 through 19. These formulae represent a relatively minor extension of Corey's[18] concept. In effect, the space occupied by gas and oil is considered as a separate porous medium in which oil is the wetting phase and gas is the nonwetting phase.

$$p_{c_{g-o}} = \frac{14.7}{((1-S_g)*400)^{.5}} \quad \ldots\ldots (14)$$

$$p_{c_{w-o}} = \frac{14.7}{(S_w*400)^{.5}} \quad \ldots\ldots (15)$$

$$k_{rg} = (S_g)^2 * (1 - (S_o + S_w)^2) \quad \ldots\ldots (16)$$

$$RKNW = (1-S_w)^2 * (1 - S_w^2) \quad \ldots\ldots (17)$$

$$k_{ro} = \left(\frac{S_o}{S_o + S_g}\right)^4 * RKNW \quad \ldots\ldots (18)$$

$$k_{rw} = (S_w)^4 \quad \ldots\ldots (19)$$

As indicated by Fig. 2, the effect of hysteresis on gas relative permeability was included. At gas saturations below 30 percent of pore space, any decrease in gas saturation causes a very rapid decline in gas relative permeability. When the gas relative permeability reaches zero, the remaining gas saturation is immobile or trapped. Any decrease in gas saturation beyond this point must be either by compression or solution effects. The gas saturation trapped is, of course, a function of initial gas saturation. To demonstrate the importance of including gas relative permeability hysteresis, comparative simulations were made including and excluding hysteresis. After flooding to a producing WOR of 200, the resulting gas saturation profiles are shown in Fig. 5. It is readily observed that, without hysteresis, the gas left in the reservoir varies from 1 to 2 percent of reservoir PV vs 28 percent when the hysteresis effect is taken into account. Since trapping of gas is necessary to derive any benefit of original gas saturation, it is essential to include the hysteresis effects to reproduce performance of natural reservoir systems.

Hysteresis effects were similarly included for the RKNW as shown in Fig. 3. At total oil and gas saturations below 44.4 percent of total pore space, any decrease in oil plus gas saturation causes a rapid decrease in the relative permeability of the total hydrocarbon phases. The basis of this work was derived from the work of Kyte et al.[4] Kyte found that the residual oil saturation, after a complete waterflood for a water-wet sand, is a linear function of trapped gas saturation. Analysis of his work showed that, after complete waterflood, the total residual saturation of hydrocarbon phases is also a linear function of the trapped gas saturation. The relationship between immobile gas saturation and residual saturation of hydrocarbon phase after waterflood from the work of Kyte is shown in Fig. 6. Curve ACB in Fig. 7 shows the relationship between the residual oil saturation and trapped gas saturation as derived by Kyte. His work indicated that there is no recovery of oil after water breakthrough for oils of low viscosity for all values of trapped gas saturations. The work of Holmgren and Morse[3] showed that waterflooding in the presence of gas saturation in excess of about 15 percent resulted in some oil being recovered after water breakthrough. Kyte's work for his viscosity oils also shows that there is some oil recovery after breakthrough. It is believed that the results from the short systems Kyte used may have been influenced by capillary end effects. This work duplicates Kyte's work insofar as ultimate oil recovery is concerned, but indicates some recovery after water breakthrough at trapped gas saturations above 13.5 percent. As shown in Fig. 7, the oil recovery at breakthrough follows Curve ACD, while ultimate oil recovery follows Curve ACB, which is identical with Kyte's results.

The validity of the model as well as the effectiveness of the grid system were verified by comparing the model performance against Buckley-Leverett fractional flow calculations. Fig. 8, which represents produced water-oil ratio vs average water saturation, shows the comparison between the Buckley-Leverett calculations and the numerical model performance. Minor differences in performance near water breakthrough can be attributed to the fact that the Buckley-Leverett method does not consider capillary pressure between phases and to numerical dispersion common to all models. After water breakthrough, performance shows a very close match between the two.

The physical reservoir model and the grid system used for this study are shown in Fig. 9. The calculations were made for a section of reservoir, 1 ft wide, 1,400 ft long and 25 ft thick. The gas, oil and water properties used for all calculations appear in Table 1.

Final material-balance errors on all simulations were less than 0.0003 percent of the fluid originally in place for oil, less than 0.002 percent for water and less than 0.2 percent for gas. Total simulation times varied from less than 30 seconds to 2.5 minutes for the one-dimensional tests. Run times for the two-dimensional simulations covering the same production history were up to 10 minutes. An IBM 360-65 computer was used for calculations.

DISCUSSION AND RESULTS

In order to eliminate solution gas drive effects from the simulated waterfloods, the simulation was conducted with constant pressure at the fluid producing end. At the start of each waterflood, pressure in all the cells was the same except for differences resulting from the gravity gradient.

Effects of Variable Water Injection Rates on the Performance of Waterflooding a One-Dimensional System

For this series of simulations the fluid saturations immediately preceding the waterfloods were (1) gas saturation - 30 percent of PV, (2) oil saturation - 50 percent and (3) water saturation - 20 percent. As shown in Fig. 9, water was injected into one end of the system at a constant rate and a constant pressure was maintained at the outlet end.

Complete waterflood performances were simulated for seven different water injection rates. Variations in the rate of water injection resulted in widely different pressure differentials across the system. The pressure differential across the system for a particular rate of water injection varied throughout the period of waterflood. At the start of water injection, pressure differentials started increasing, passed through a maximum and, as the oil bank was produced, started decreasing. Table 2 summarizes the waterflood data for all the water injection rates simulated in the study. In all the floods, the simulation continued until the producing WOR reached 200.

Figs. 10 through 13 show the gas and oil saturation profiles for seven different rates of water injection at four different values of cumulative water injected.

Fig. 10 shows oil and gas saturation profiles existing in the systems after 0.125 PV of water had been injected. It is observed that, at high injection rates, a significant amount of free gas has disappeared by being forced into solution in the oil between 350 and 1,225 ft, while free gas is present between 0 and 350 ft. The oil saturation profile for high rates indicates that a sharp oil bank exists between 525 and 1,050 ft, while the oil saturation from 0 to 350 ft is the same as it was at the start of the waterflood. However, at low rates, gas has been trapped and maintained at about 26 to 27 percent saturation and oil from 350 ft to 1,225 ft has been displaced toward the producing end.

Fig. 11 shows the saturation profiles at a cumulative water injection of 0.25 PV of water. Except for the very low rates, all gas present in the system is trapped. At high water injection rates the gas saturation has been reduced to zero in some sections, while in others it has been reduced below the gas saturation at which gas permeability is zero. The gas trapped by the advancing oil bank is compressed and forced into solution in the oil by increasing pressure. Gas saturation profiles are fairly uniform for low water injection rates. Oil saturation profiles show that, at increasing water injection rates, a sharper oil bank results ahead of the waterflood.

Fig. 12 represents saturation profiles after 0.375 PV of water were injected. Gas saturation profiles are not significantly different from those of Fig. 11 except that some more gas has been forced into the solution by increasing pressures. For the high injection rates, the section between 700 and 1,225 ft has been flooded to the irreducible oil saturation, but a sharp oil bank still exists near the producing end. At low rates of water injection, there is no definite "oil bank" and the whole system is contributing to oil production.

Fig. 13 represents saturation profiles after 0.5 PV of water were injected. Gas saturation profiles are almost identical to those in Fig. 12. All oil saturations, except those near the producing end, have reached the irreducible level.

Fig. 14 shows the gas and oil saturation profiles at the end of waterflooding to a WOR of 200. Also shown in this figure is the saturation profile for a simulated flood in which no gas saturation was present prior to flooding. In the absence of gas saturation the residual oil saturation following the waterflood is seen to be 28 percent of PV. If 28 percent gas saturation is trapped, maintained during the waterflood, and the system flooded to an infinite water-oil ratio, the residual oil saturation is reduced to 14.4 percent.

At high water injection rates, the gas saturation in some sections of the system is reduced to zero. In other parts of the system gas saturation is reduced below the 28 percent level at which it was trapped by the oil bank. The net result is that in parts of the system no benefits or only partial benefits of trapped gas saturation are derived at high injection rates. At high rates residual oil saturations are higher than those for low injection rates where very little volume of gas goes back into solution.

Figs. 15 and 16 show the oil saturation profiles at water injection rates of 0.0107 and 12.84 B/D. Profiles are shown for different volumes of water injected. As shown by Fig. 15, at the low rate very little oil banking is evident. After 1.75 PV of water had been injected, the produced WOR is 200. The oil saturation profile for 1.75 PV of water injected indicates that most of the system has reached the irreducible oil saturation corresponding to the gas saturation present. Fig. 16 shows that at high rate a sharp oil bank develops. Part of the system has reached irreducible oil saturation before the oil bank breakthrough. Oil recovery after breakthrough is small. After injection of 0.99 PV of water the produced WOR was 200. The saturation profile for 0.99PV of water injected indicates that no benefit of the original gas saturation has been derived in the part of the system from 350 ft to 1,225 ft.

Fig. 17 illustrates, for all injection rates, the variation of average gas and oil saturations with cumulative water injected. Average gas saturation is an essentially linear function of pore volumes of water injected at the start of the flood. The average gas saturation passes through a minimum and increases slightly near the end of the flood. After water breakthrough, the pressure in the system starts to decrease, resulting in the liberation of solution gas from the residual oil and expansion of the trapped gas. The average oil saturation increases above that present at the start of the waterflood in the high water injection rate simulations. This is the result of gas being forced into solution in the oil and, hence, an increasing oil reservoir volume factor. At low injection rates, only a negligible amount of gas goes into solution in the oil so the average oil saturation starts decreasing from the start of water injection. At all values of cumulative water injected, the average oil saturation of the system increases as injection rate increases. This is simply because the higher rates of water injection cause pressure increases that diminish the amount of gas saturation present upon arrival of the waterflood front.

Fig. 18 shows the oil recovered as a fraction of oil initially in place as related to cumulative water injected. At low flooding rates oil production starts when less cumulative water has been injected than for higher injection rates. For all amounts of cumulative water injected the oil recovery is highest for the lowest rate of water injection. This figure also indicates that oil recovery after water breakthrough is almost negligible for the high injection rate floods.

Fig. 19 indicates the variations in ultimate oil recovery (at a WOR of 200) with water injection rates. For the system under study ultimate oil recovered varies from 71.5 percent to 50.5 percent of oil originally in place. Initial slope of the curve is steep and then tends to level off. Once increasing injection rates have caused pressures to increase enough to put all gas into solution, further increases in injection rate have no further effect.

Effects of Variable Water Injection Rates on the Performance of Two-Dimensional Waterfloods

In oil-producing reservoirs where gravity forces have a significant effect, gas has a tendency to migrate to the top of the producing section. Thus, there will be more gas available to be trapped in the upper levels than in the bottom of the section. For the two-dimensional floods reported here, the physical model simulated is shown in Fig. 9. Gas saturations shown were those resulting from a solution gas drive simulation reported by Morse and Whiting.[15] Specifically, saturations are those resulting from a solution gas drive from 1,791.4 psi to 1,500 psi at an oil-production rate of 0.1 STB/D. At the start of waterflood simulations, water saturation was 20 percent of PV in the bottom section of the reservoir and water saturations in the rest of the reservoir were in static capillary pressure equilibrium.

Simulations were made for three different rates of water injection, and flooding was continued until the produced WOR reached 200. The gravity pressure differential between water and oil from top to bottom of the system was 2.23 psi. Table 3 summarizes the waterflood data for all the three water injection rates simulated in this study.

Fig. 20 illustrates the movement of the waterflood front for different rates of water injection. The position of the flood fronts has been represented after about 14, 28, 42 and 56 percent of the oil initially in place has been produced. Also represented is the position of the flood front at a produced WOR of 200 for each of the runs. The line denoted as the flood front shows the boundary of the completely flooded zone; that is, the oil saturation has reached the value at which oil permeability is zero.

There is no significant difference of oil recoveries between the water injection rate of 0.1 and 0.5 B/D. For both of the floods, the pressure differentials across the system are substantially greater than the gravity head between water and oil. There is more residual oil left in the outlet top corner area for 0.1 B/D flood than for 0.5 B/D flood. Water breakthrough occurs starting with the bottom section first. However, at a WOR of 200, almost all of the reservoir has been flooded.

For the water injection rate of 0.001 B/D, the resulting pressure differential across the system is less than the water-oil gravity head and the percentage of oil recovered is much less than observed in the higher rate floods. Injected water preferentially floods the bottom-most section of the system. Flooding of upper sections of the reservoir takes place from the bottom upward, rather than horizontally. At a produced WOR of 200, an appreciable fraction of the upper part of the system is left unflooded.

It must be pointed out that the above results are quantitatively applicable only to the reservoir simulated. The exact effect of water injection rate will be affected to a marked degree by fluid properties such as solubility, viscosity and shrinkage as well as by relative permeability properties and the flood pattern. Gravity effects will increase with the thickness of reservoirs flooded.

CONCLUSIONS

The behavior of one-dimensional horizontal waterfloods has been investigated under a very wide range of water injection rates. Importance of gravitational forces on the performance of waterflooding has been studied in a series of two-dimensional simulations. Conclusions of this work are as follows.

1. Numerical models can be used to duplicate quantitatively the effects of free gas saturation on performance of laboratory waterfloods.

2. In the absence of gravity the effects on waterflood oil recovery of an initial free gas phase are sensitive to flooding rate over a wide range of rates. In this range, oil recovered decreases with increasing rate.

3. At flooding rates higher than a certain level (depending on reservoir and fluid characteristics) no beneficial effect of an initial free gas phase is noted. In this rate range all free gas is dissolved prior to the arrival of the waterflood front.

4. When gravity effects are considered, lower flooding rates tend toward lower oil recoveries over a certain range of flooding rates.

5. An optimum waterflooding rate is indicated for any given horizontal oil reservoir because of the opposing effects of gravity and initial free gas saturation.

NOMENCLATURE

u_g = gas flow velocity
u_o = oil flow velocity
u_w = water flow velocity
q_g = gas production or injection rate
q_o = oil production or injection rate
q_w = water production or injection rate
S = saturation expressed as a fraction of the total pore space
S_g = gas saturation
S_o = oil saturation
S_w = water saturation
R_s = gas solubility in oil
A9 = factor including terms for production, injection, gravity and capillary pressure forces
A8 = factor including all compressibility terms
O = coefficient of pressure differential between blocks
O_x^+ = coefficient of pressure differential between the element under consideration and the adjacent block in the direction of increasing x
p = pressure
Δp = pressure differential between adjacent flow blocks
$p_{c_{w-o}}$ = capillary pressure between the water and oil phases
$p_{c_{g-o}}$ = capillary pressure between the gas and oil phases
k = single-phase permeability
k_{rg} = relative permeability to gas-fraction of single-phase permeability
k_{rgx} = relative permeability to gas in the x direction
RKNW = relative permeability to a single hydrocarbon phase of saturation equal to the sum of oil and gas saturations
μ_g = gas viscosity
μ_o = oil viscosity
μ_w = water viscosity
ρ_g = pressure gradient due to gas density
ρ_o = pressure gradient due to oil density
ρ_w = pressure gradient due to water density

Lower Case Letters

g = gas
o = oil
w = water
x = horizontal direction
z = vertical direction
t_o = time at start of calculation interval
t_1 = time at end of calculation interval
+ = increasing x or z direction
− = decreasing x or z direction

REFERENCES

1. Russell, William L.: "Some Preliminary Experiments on Oil Recovery Process," Circular 8, New York State Museum (Nov., 1932).
2. Breston, Joseph N.: "Injection of Natural Gas Before and During Waterflooding," Prod. Monthly (June, 1952) 16.
3. Holmgren, C. R. and Morse, R. A.: "Effect of Free Gas Saturation on Oil Recovery by Waterflooding," Trans., AIME (1951) 192, 135-140.
4. Kyte, J. R., Stanclift, R. J., Jr., Stephan, S. C., Jr., Rapoport, L. A.: "Mechanism of Waterflooding in Presence of Free Gas," Trans., AIME (1956) 207, 215-221.
5. Schiffman, Louis and Breston, Joseph N.: "The Effect of Gas on Recovery When Waterflooding Long Cores," Prod. Monthly (Jan., 1950) 11.
6. Calhoun, John C., Jr.: "The Injection of Gas as an Aid in Waterflooding," Prod. Monthly (Feb., 1953) 32.
7. Pfister, R. J.: "More Oil from Spent Water Drives by Intermittent Air or Gas Injection," Prod. Monthly (Sept., 1947) 10.
8. Holmgren, C. R.: "Some Results of Gas and Water Drives on a Long Core," Trans., AIME (1949) 179, 103-118.
9. Dyes, A. B.: "Production of Water-Driven Reservoirs Below Their Bubble Point," Trans., AIME (1954) 201, 240-244.
10. Bass, D. M.: "Waterflooding at Pressures Above and Below the Bubble Point," MS Thesis, Texas A&M U., College Station, Tex. (1955).
11. Nielsen, R. F.: "Review of Studies on Factors Affecting Recovery by Water Flood," Prod. Monthly (Dec., 1950) 19.
12. Arnold, M. D.: "Effects of Fluid Properties and Initial Gas Saturation on Oil Recovery by Water Flooding," MS Thesis, Texas A&M U., College Station, Tex. (1959).
13. Buckley, S. E. and Leverett, M. C.: "Mechanism of Fluid Displacement in Sands," Trans., AIME (1941) 146, 107-116.
14. Heath, W. A.: "Gas Injection Prior to Water Flooding in the Mid-Continent Area," Prod. Monthly (Feb., 1953) 40.
15. Morse, R. A. and Whiting, R. L.: "A Numerical Model Study of Gravitational Effects and Production Rate on Solution Gas Drive Performance of Oil Reservoirs," J. Pet. Tech. (May, 1970) 625-636.
16. Breitenbach, E. A., Thurnau, D. H. and van Poollen, H. K.: "The Fluid Flow Simulation Equations," Paper SPE 2020 presented at Symposium on Numerical Simulation of Reservoir Performance, Dallas, April 22-23, 1968.
17. Breitenbach, E. A., Thurnau, D. H. and van Poollen, H. K.: "Solution of the Immiscible Fluid Flow Simulation Equations," Soc. Pet. Eng. J. (June, 1969) 155-169.
18. Corey, A. T.: "The Interrelation Between Gas and Oil Relative Permeabilities," Prod. Monthly (1954) 38.

TABLE 1 - FLUID CHARACTERISTICS

Pressure Psi	Reservoir Volume Factor: Gas MCF / Res. Bbl	Reservoir Volume Factor: Oil Res. Bbl. / STB	Density Gradient: Gas Psi/Ft.	Density Gradient: Oil Psi/Ft.	Gas Solubility in Oil: MCF/STB	Viscosity-Centipoise: Gas	Viscosity-Centipoise: Oil
2000	1.1695	1.2676	0.0784	0.3204	0.5800	0.0167	1.3593
1825	1.1191	1.2698	0.0733	0.3199	0.5800	0.0170	1.3505
1600	0.9807	1.2447	0.0641	0.3232	0.5213	0.0161	1.3853
1200	0.7149	1.2005	0.0467	0.3292	0.4120	0.0144	1.4537
800	0.4412	1.1573	0.0288	0.3353	0.3027	0.0133	1.6147
400	0.1948	1.1089	0.0127	0.3431	0.1864	0.0119	2.0723
100	0.0410	1.0441	0.0027	0.3569	0.0667	0.0110	3.2476

Note: Gas solubility in water is zero. Water has a formation volume factor of 1.0 Res. Bbl/STB and water viscosity is 0.8 times oil viscosity.

TABLE 2 - SUMMARY OF ONE-DIMENSIONAL FLOODING DATA

Rate of Water Injection Bbls/Day	Maximum Pressure Differential Psi	Average Reservoir Properties at Terminal Water-Oil Ratio of 200: Gas Saturation	Oil Saturation	Water Saturation	Pressure	Oil Recovered at Water - Oil Ratio of 200: Fraction of Oil in Place	Fraction of Pore Volume
0.0107	11.88	0.2761	0.1485	0.5754	503.65	0.7031	0.3516
0.107	92.04	0.2525	0.1593	0.5882	532.81	0.6813	0.3407
0.535	291.25	0.1896	0.1887	0.6217	637.48	0.6283	0.3142
1.07	457.37	0.1487	0.2088	0.6425	736.80	0.5931	0.2966
2.14	725.64	0.1030	0.2300	0.6670	891.36	0.5517	0.2759
6.42	1665.52	0.0507	0.2557	0.6936	1410.79	0.5190	0.2597
12.84	3017.12	0.0390	0.2610	0.7000	2171.41	0.5040	0.2521

Note: For all water floods: Original Gas Saturation = 0.30 of pore volume, Oil Saturation = 0.50, Water Saturation = 0.20 and Pressure - 500 psi.

TABLE 3 - SUMMARY OF TWO-DIMENSIONAL FLOODING DATA

Rate of Water Injection Bbl/Day	Maximum Horizontal Pressure Differential Lower Most Section-Psi	Average Reservoir Properties at Terminal Water Oil Ratio of 200: Gas Saturation Fraction Pore Volume	Oil Saturation Fraction Pore Volume	Water Saturation Fraction Pore Volume	Pressure	Oil Recovered Water Oil Ratio of 200: Fraction of Oil in Place	Fraction of Pore Volume
0.001	2.807	0.0597	0.3463	0.5940	1505.14	0.5779	0.4768
0.1	23.726	0.0567	0.2554	0.6879	1514.03	0.6900	0.5682
0.5	111.573	0.0530	0.2552	0.6918	1557.73	0.6915	0.5692

Note: For all Water Floods: Original Average Gas Saturation = 0.0613 of Pore Volume, Average Oil Saturation = 0.8205, Average Water Saturation = 0.1182 and Average Pressure = 1504.34 psia.

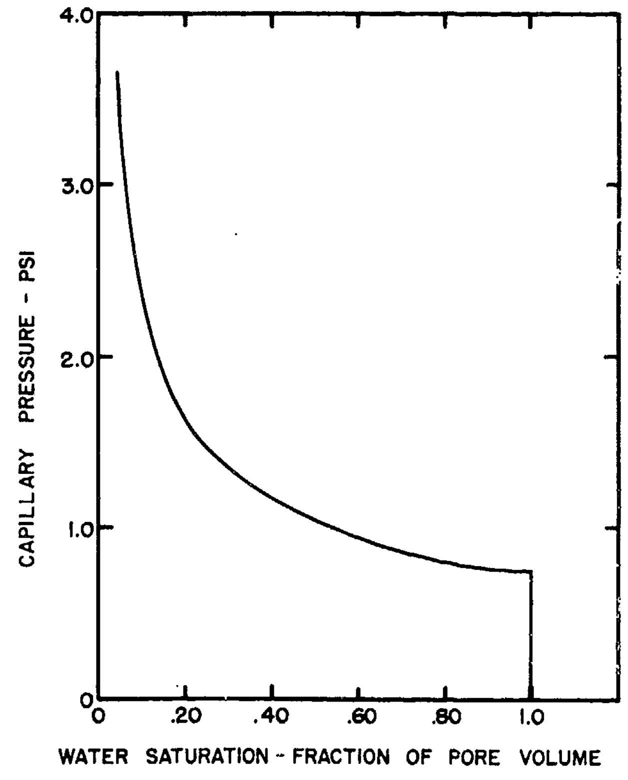

Fig. 1 - Water-oil capillary pressure curve.

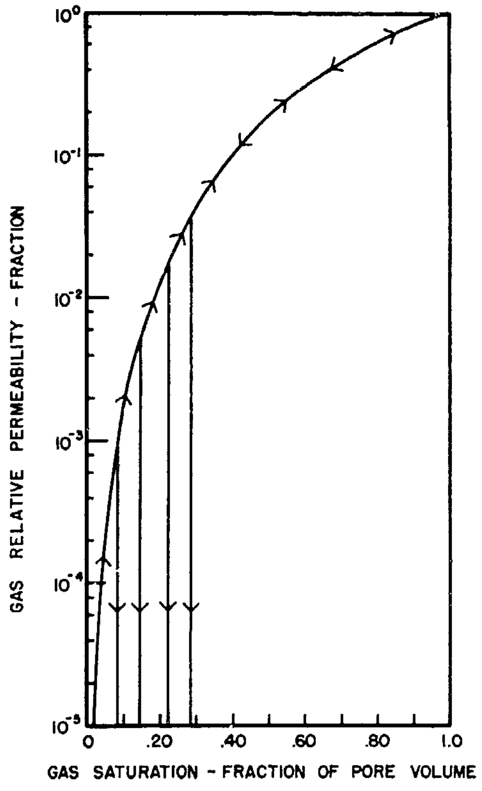

Fig. 2 - Relationship between gas relative permeability and gas saturation.

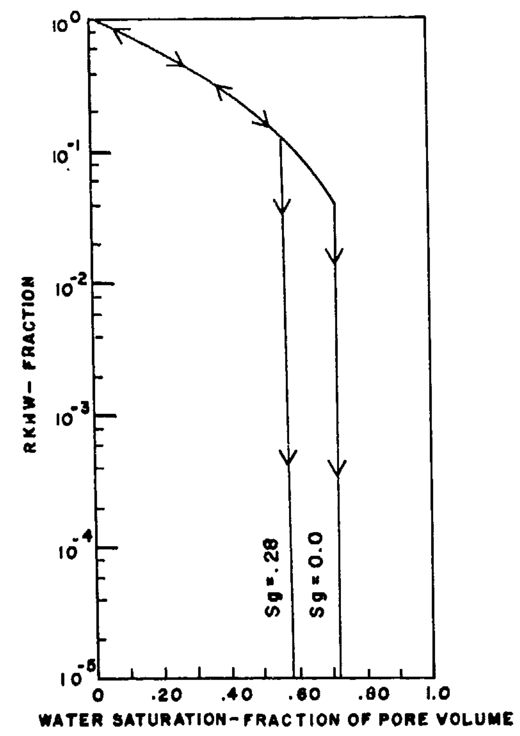

Fig. 3 - Relationship between RKNW and water saturation.

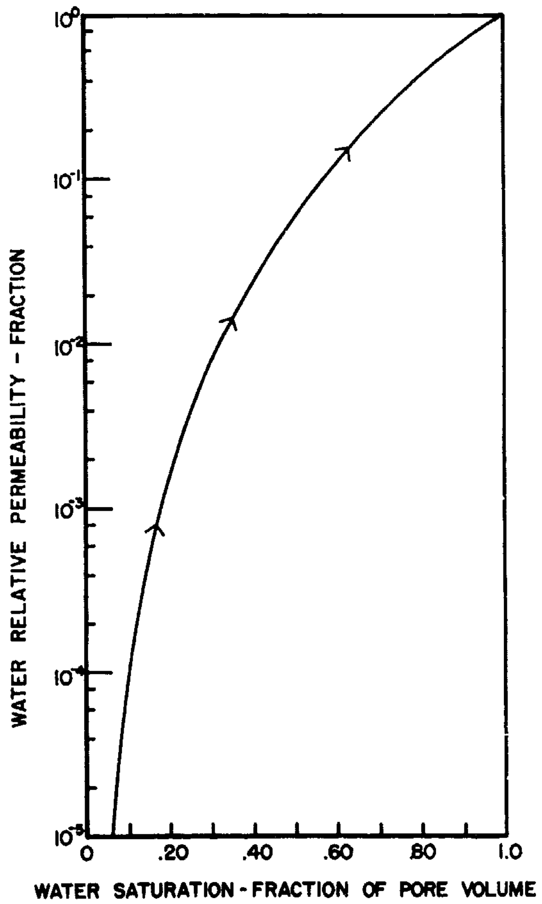

Fig. 4 - Relationship between water relative permeability and water saturation.

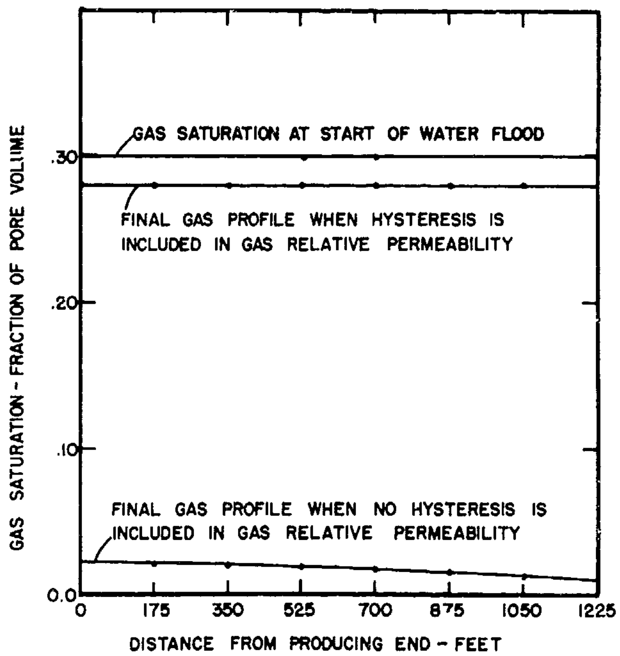

Fig. [illegible] - Gas saturation profiles after waterflood to water-oil ratio of [illegible].

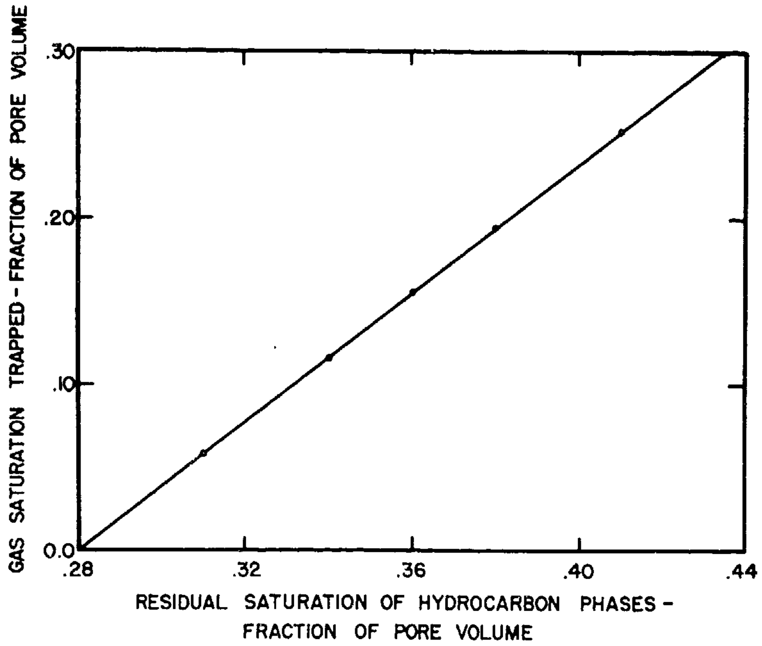

Fig. 6 - Relationship between gas trapped and total residual saturation of hydrocarbon phases (oil plus gas).

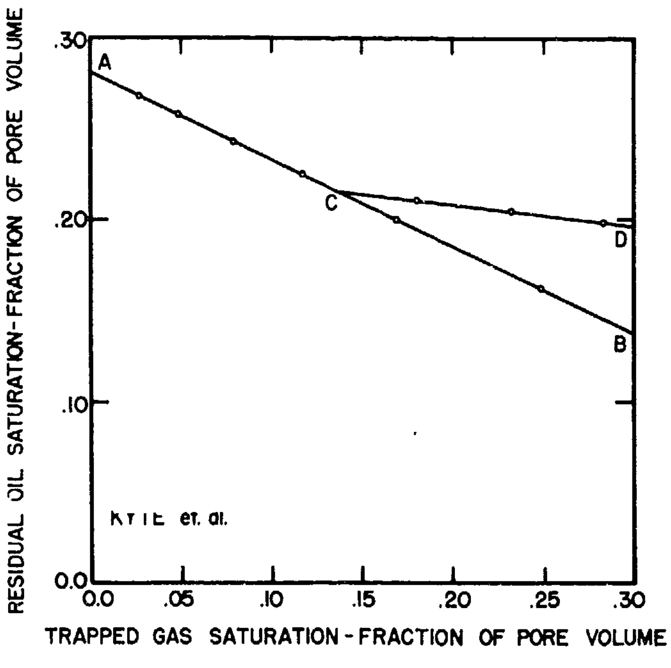

Fig. 7 - Relationship between trapped gas and residual oil saturation for light oil (1.4 cp viscosity) as presented by Kyte, et al.

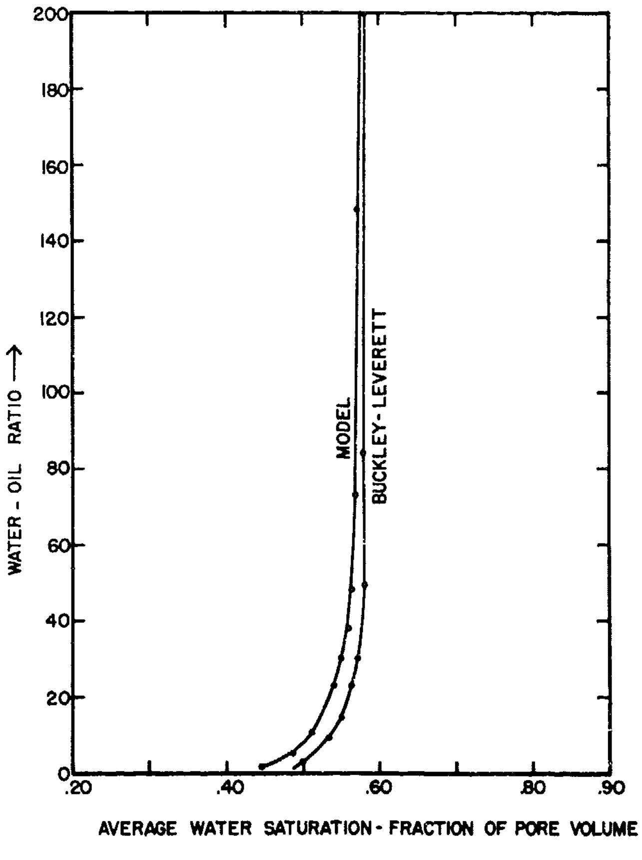

Fig. 8 - Comparison of predictions by Buckley-Leverett calculations and numerical model for one-dimensional study.

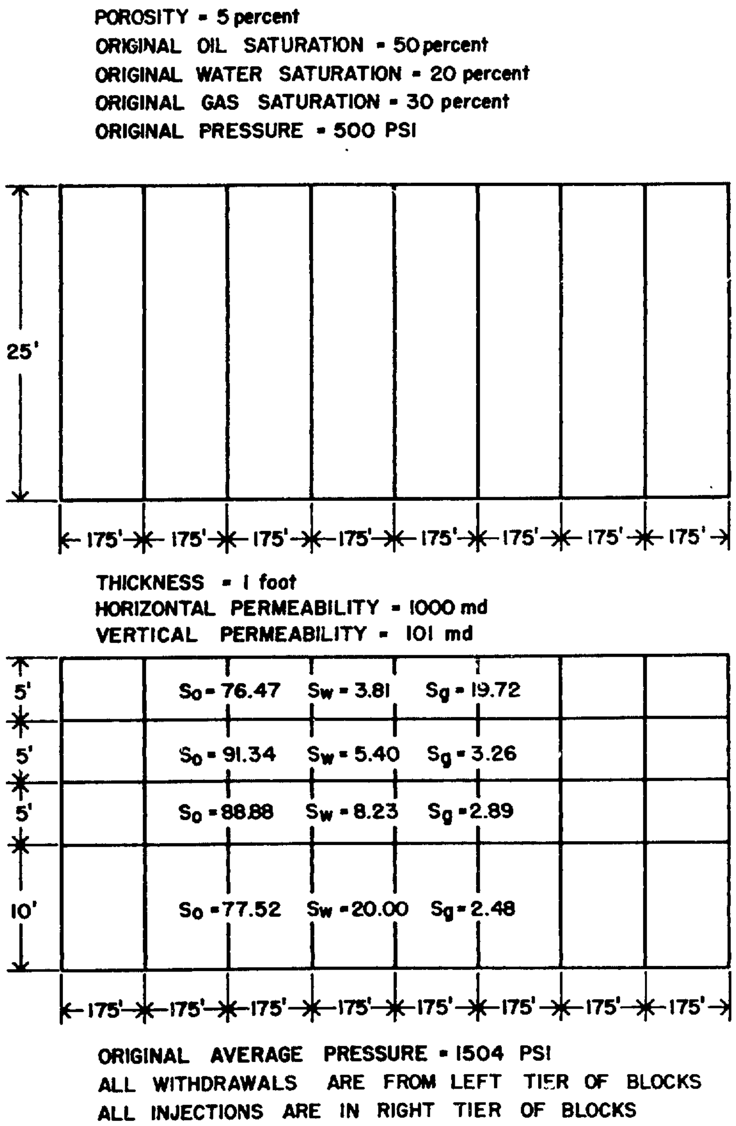

Fig. 9 - Diagrams of model reservoirs simulated.

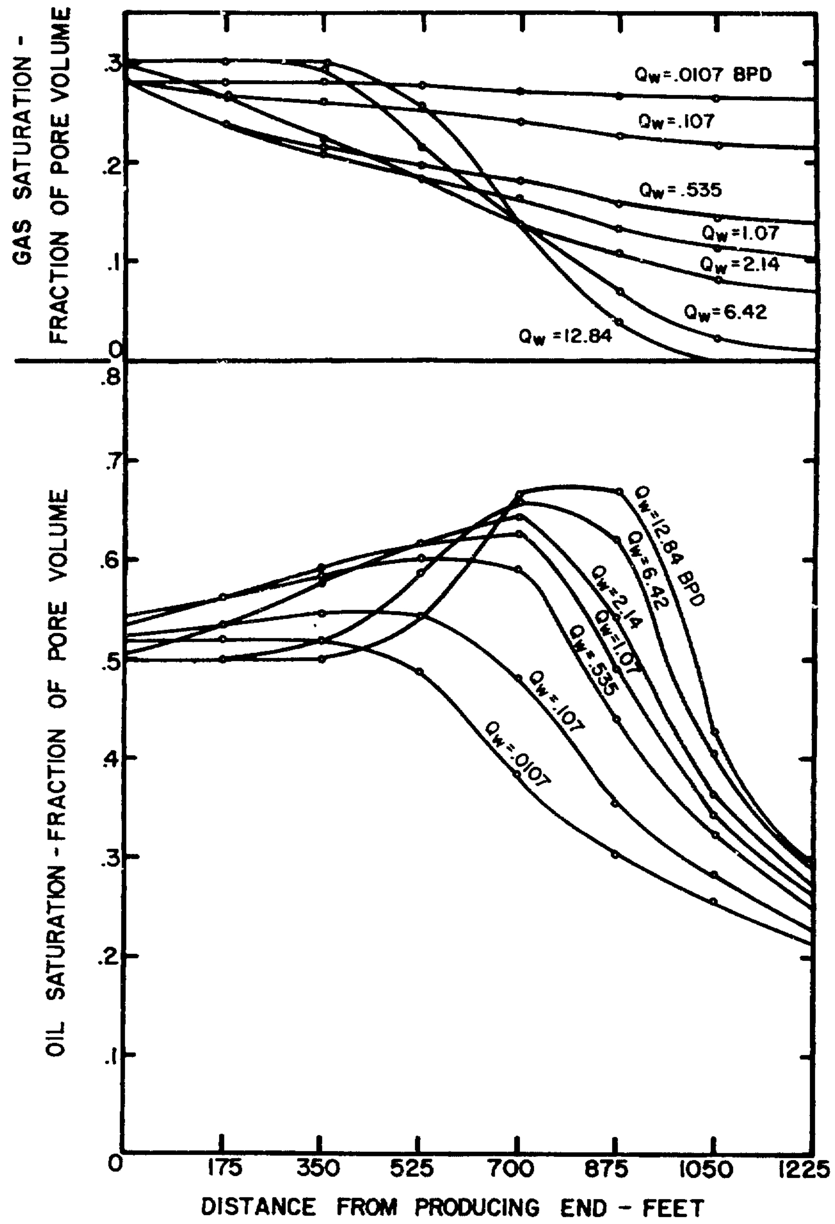

Fig. 10 - Gas and oil saturation profiles at 0.125 PV of water injected.

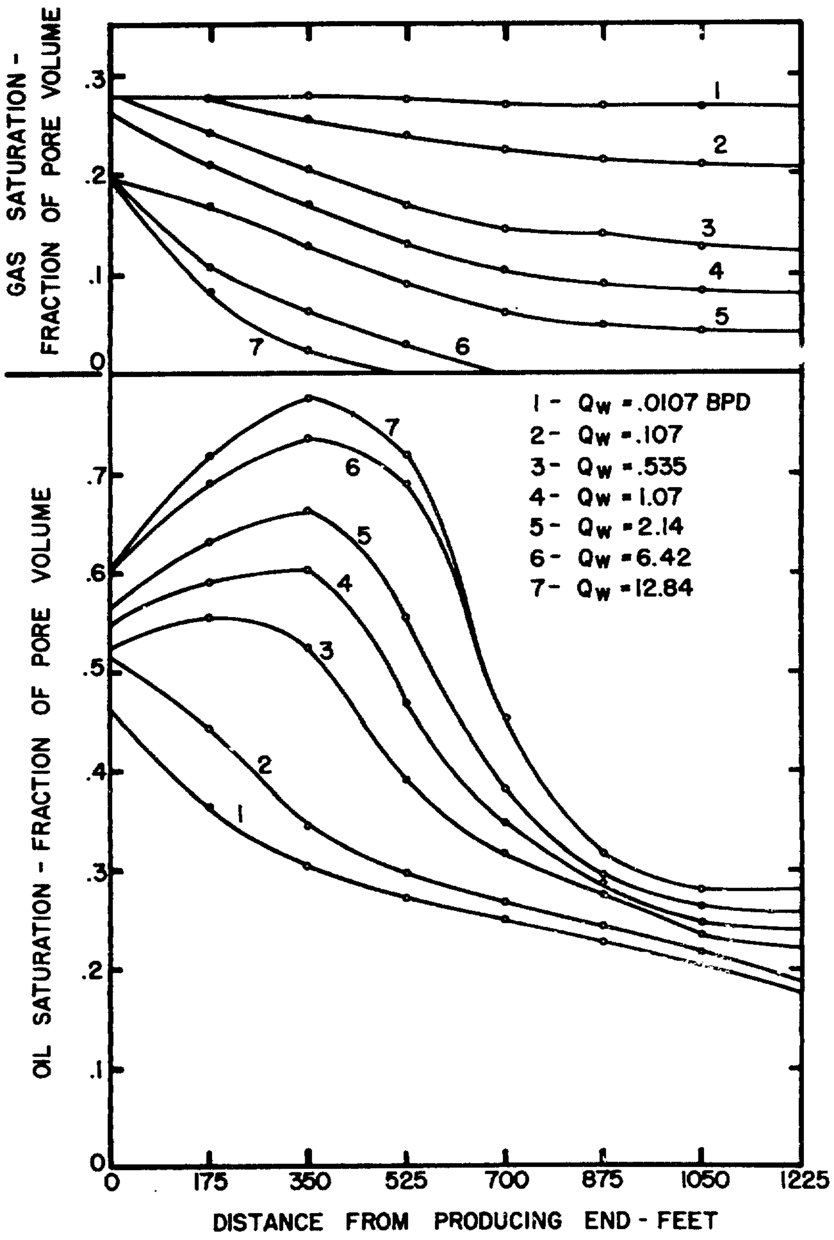

Fig. 11 - Gas and oil saturation profiles at 0.25 PV of water injected.

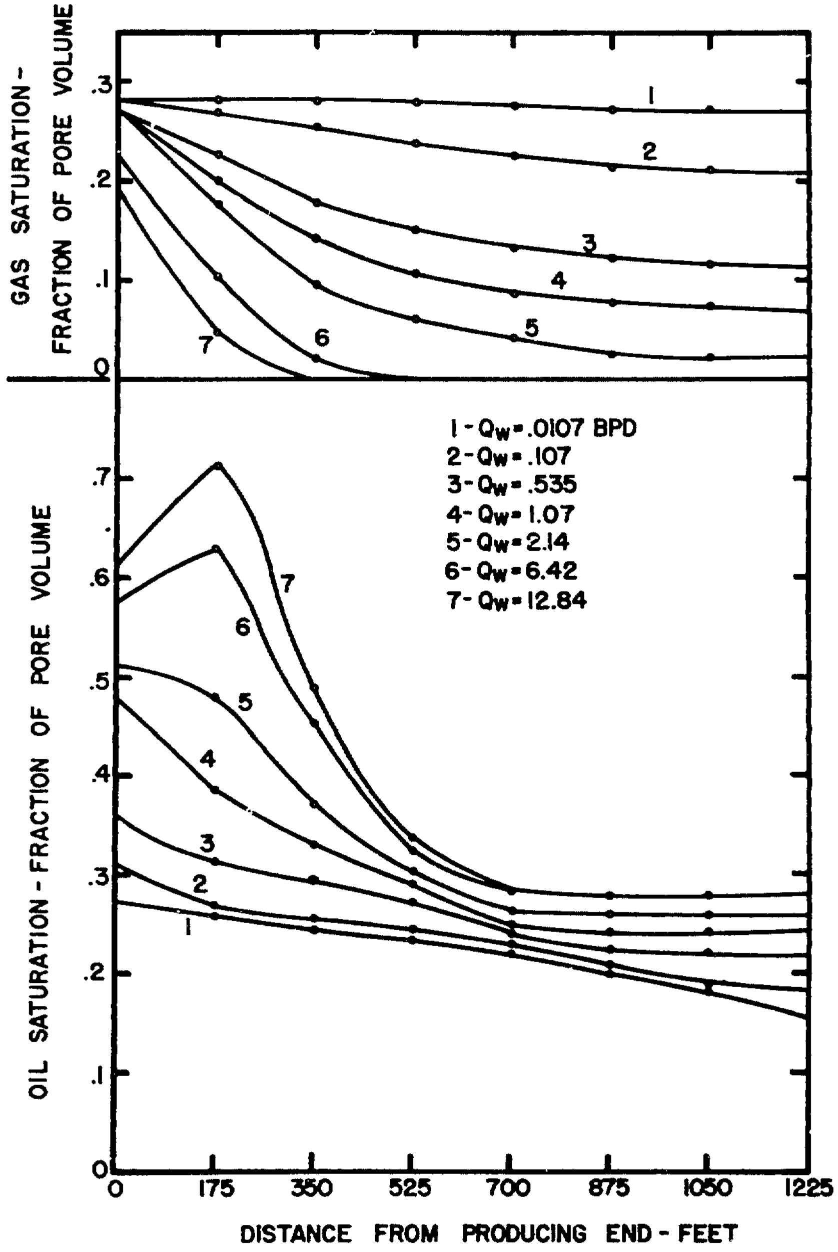

Fig. 12 - Gas and oil saturation profiles at 0.375 PV of water injected.

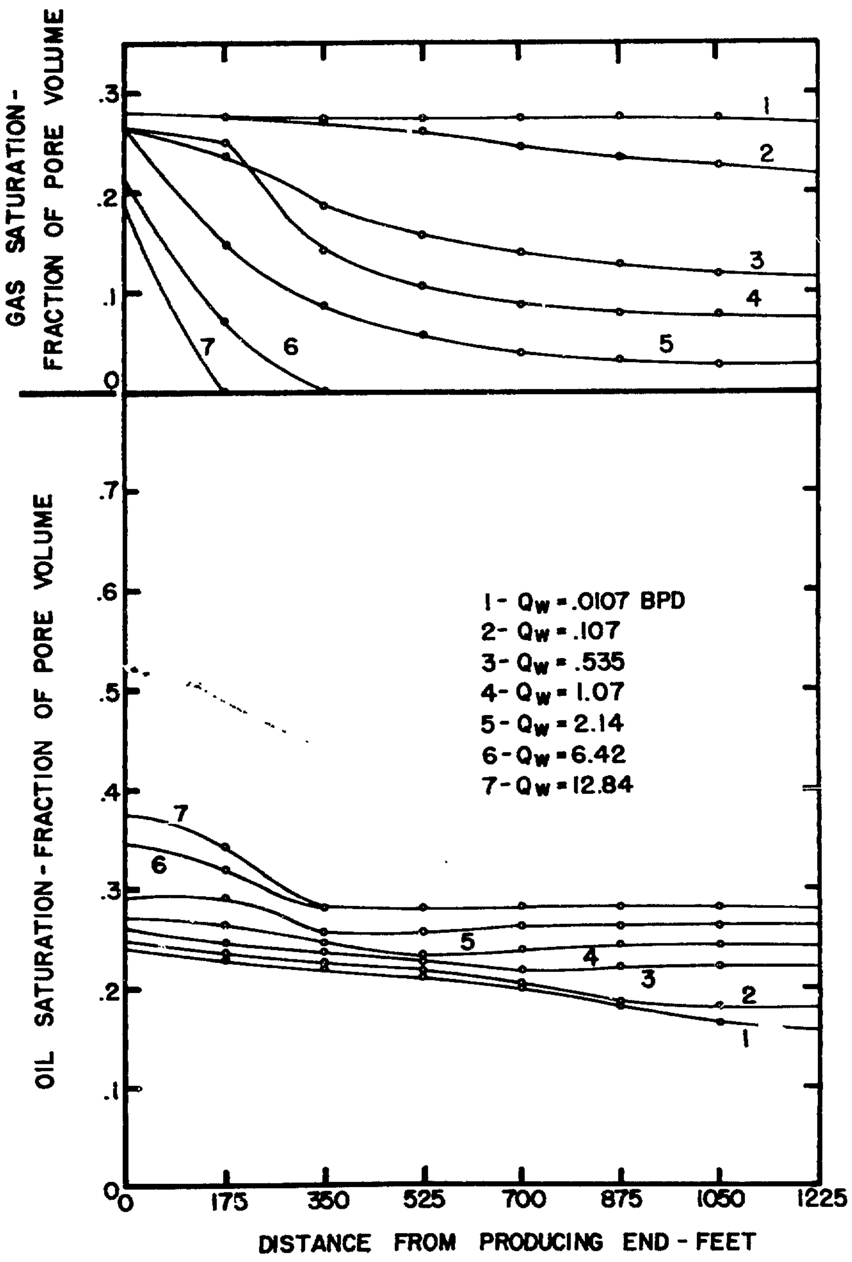

Fig. 13 - Gas and oil saturation profiles at 0.5 PV of water injected.

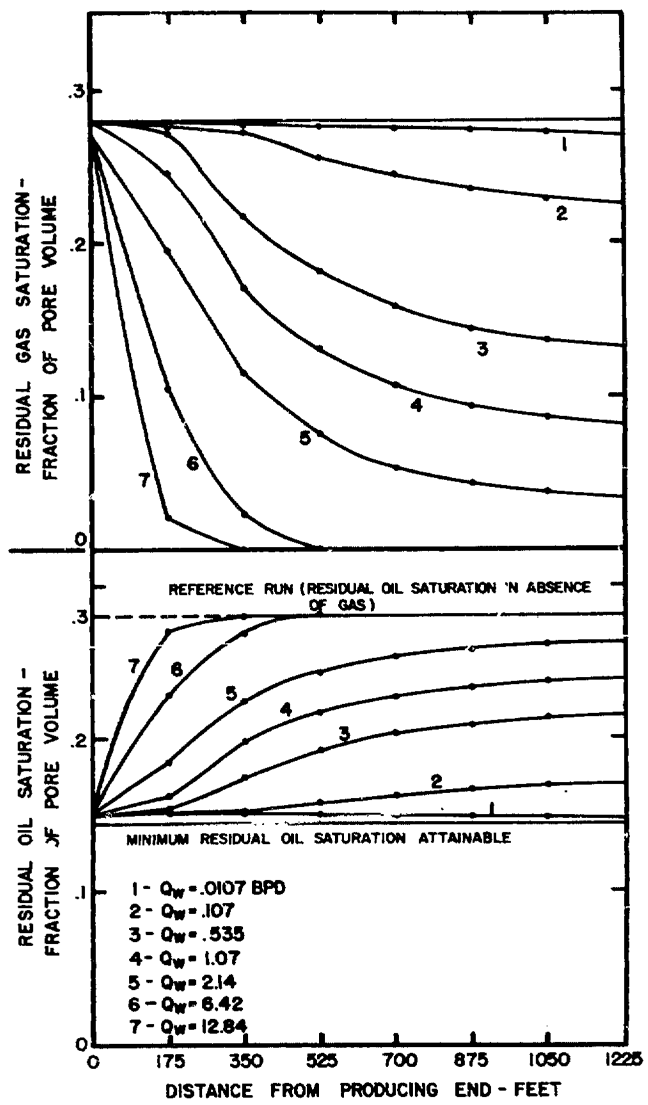

Fig. 14 - Residual gas and oil saturation profiles at water-oil ratio of 200 for different injection rates.

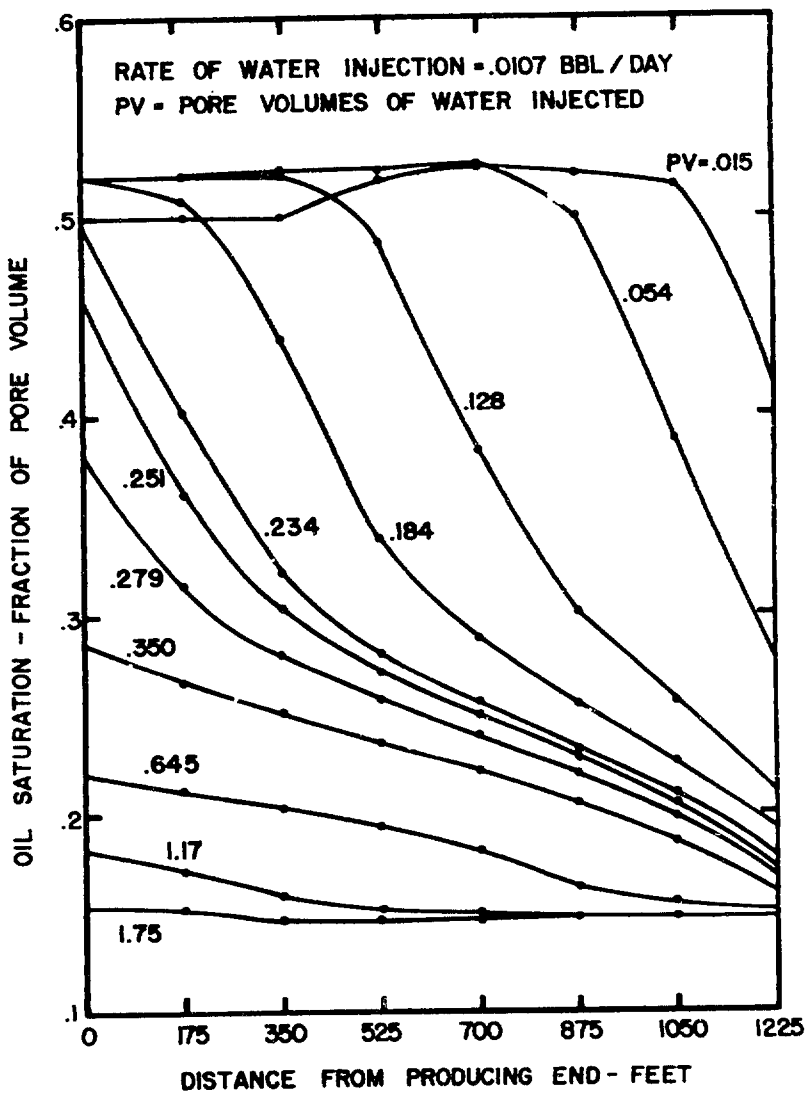

Fig. 15 - Oil saturation profiles at low injection rate.

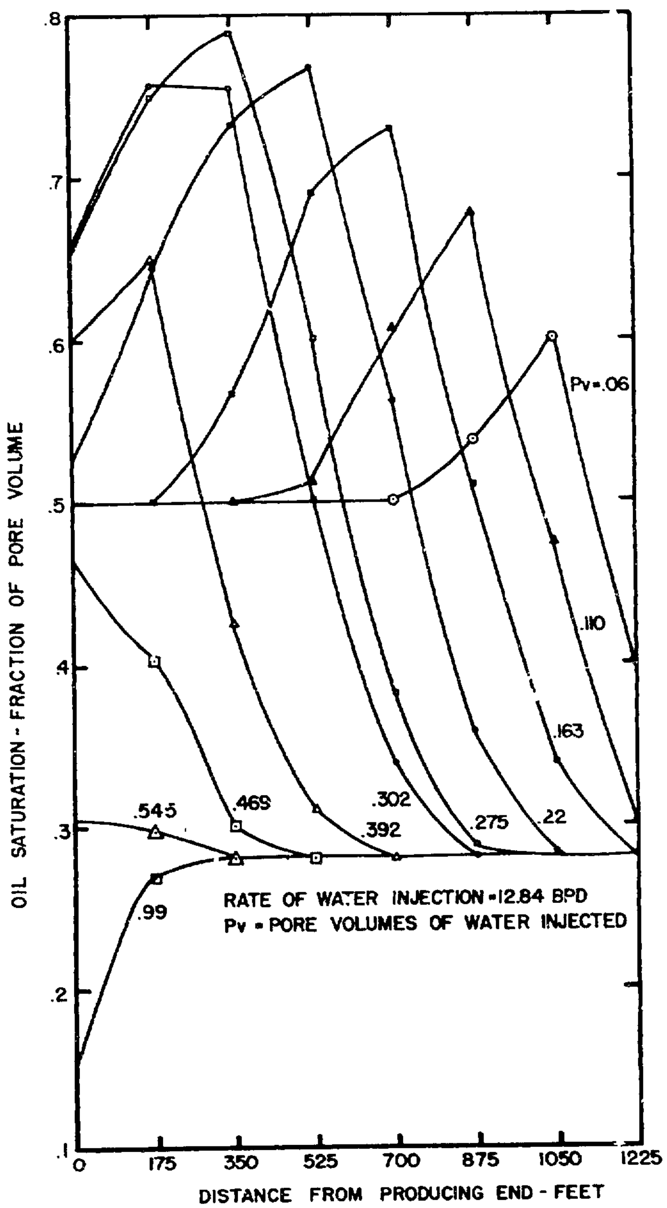

Fig. 16 - Oil saturation profile at high injection rate.

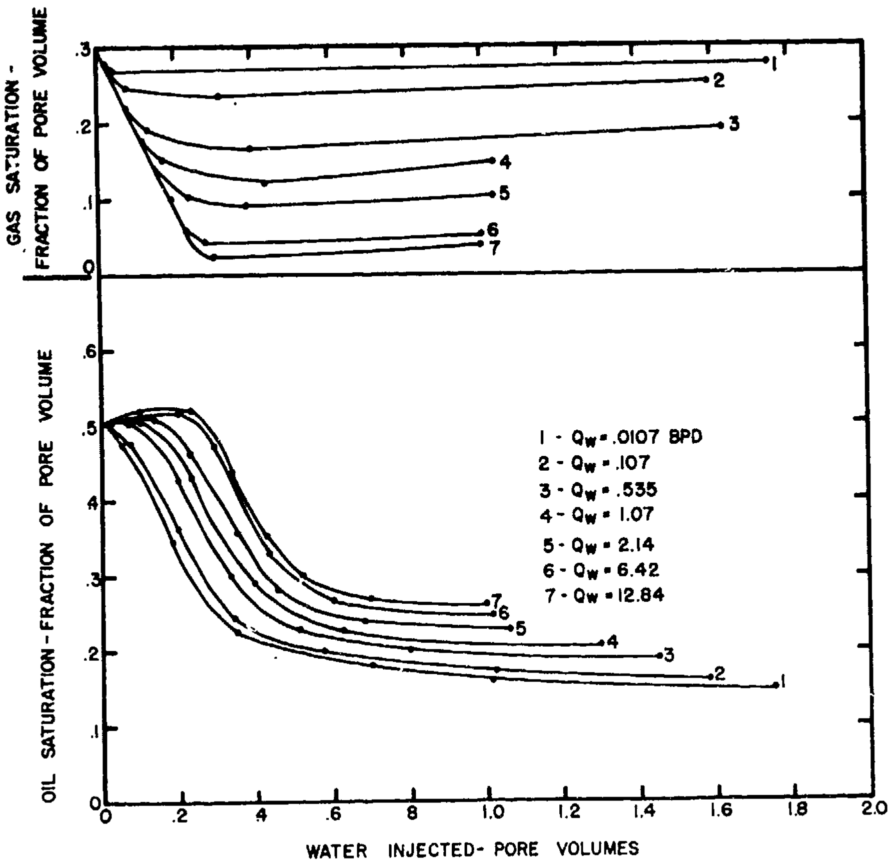

Fig. 17 - Variation of average oil and gas saturations with cumulative water injected and flooding rate.

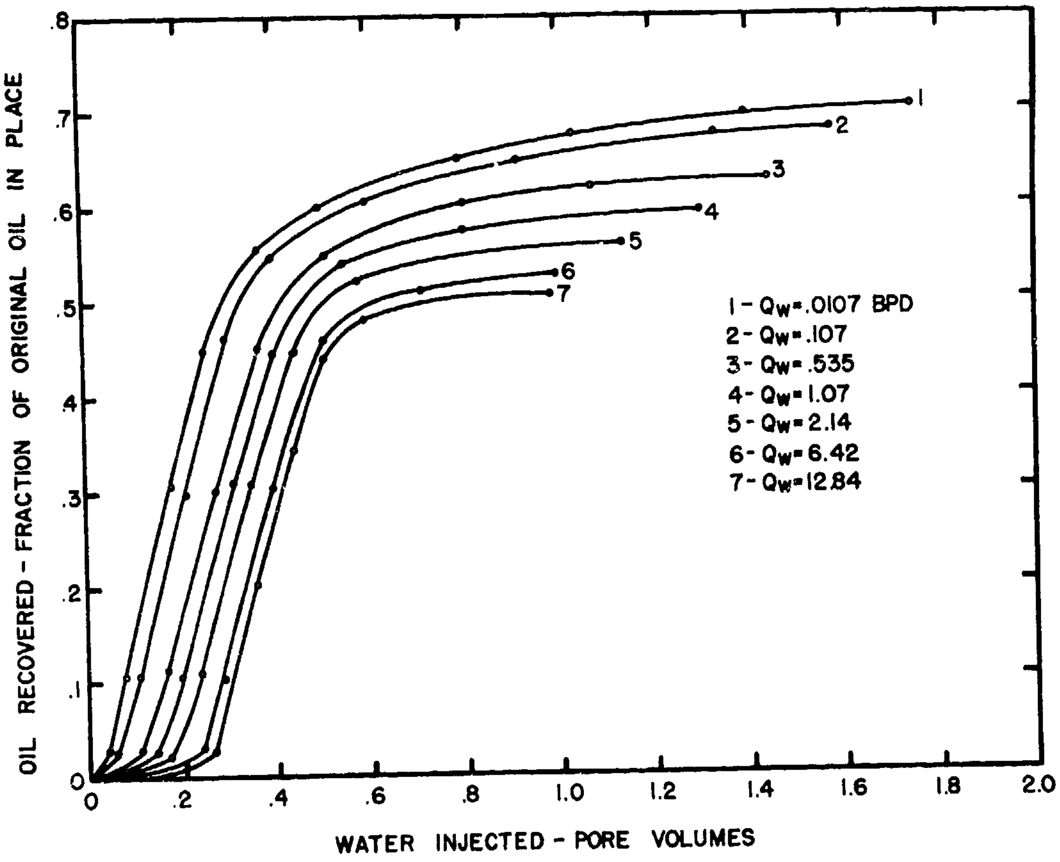

Fig. 18 - Relationship between oil recovered and water injected at different injection rates.

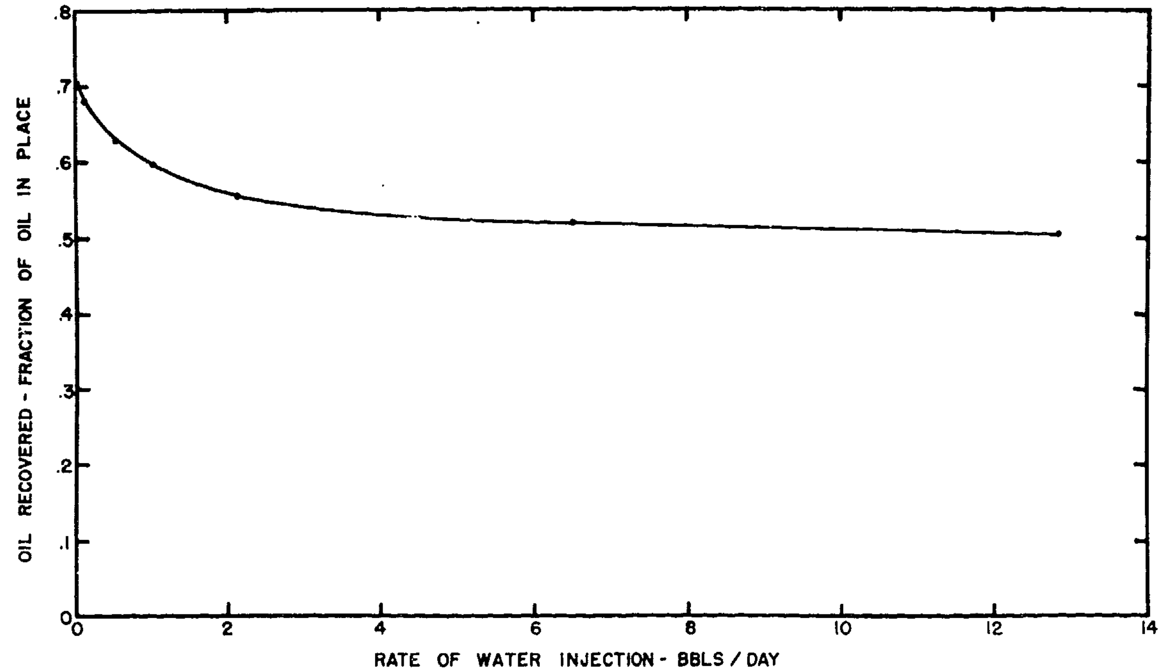

Fig. 19 - Relationship between oil recovered and rate of injection.

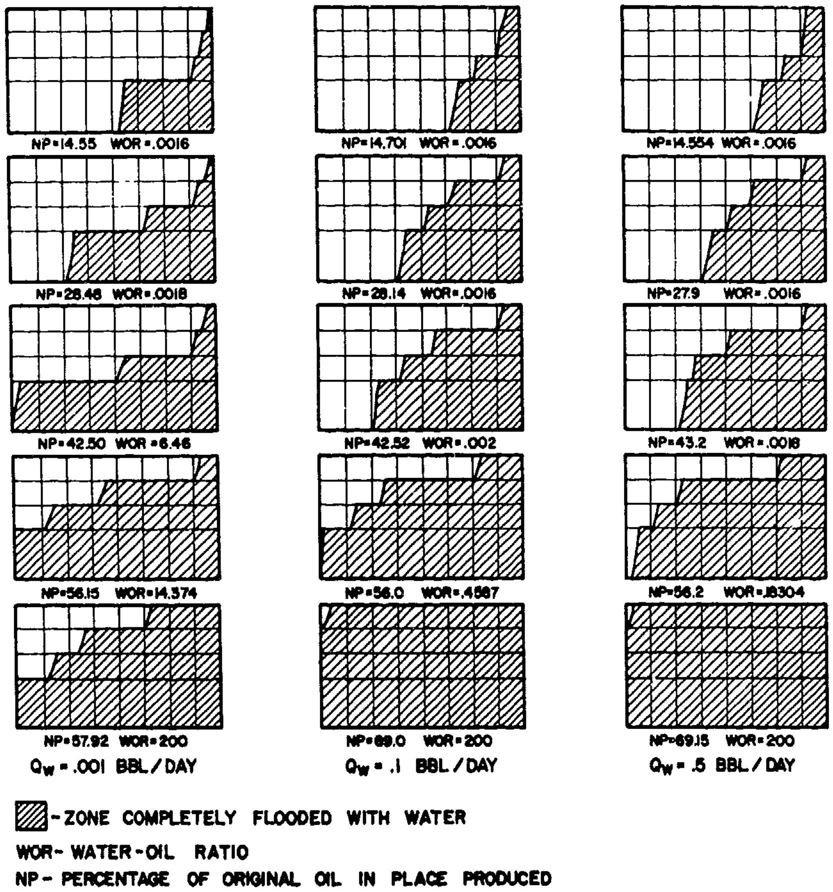

Fig. 20 - Flood fronts for different rates of water injection at different percentages of oil produced.